Modification of biochar with carbon nanotubes for potential application as an advanced CO_2 adsorbent

Luis González[a], Boris Ildusovich-Kharisov[a]* (0000-0001-7082-9357), Yolanda Peña Méndez[a] (0000-0003-3706-1504) y Oxana Vasilievna-Kharissova[a] (0000-0002-0795-9420)

[a]*Universidad Autónoma de Nuevo León, Ave. Universidad s/n, San Nicolás de los Garza, N.L. 66455, Mexico.*
**e-mail de autor responsible: bkhariss@hotmail.com.*

Recibido 15 de marzo 2026, Aceptado 10 de abril 2026

Abstract
In the present work, biochar composites were produced with multiwall carbon nanotubes, MWCNT's. The composites were characterized by Fourier transform infrared spectroscopy (FT-IR), X-ray diffraction (XRD) and surface area analysis (BET) techniques to evaluate the effect of the modifications on the adsorption capacity of CO_2. The objective of this work is to obtain a biochar-based composite with a CO_2 adsorption capacity 10% higher than that of unmodified biochar (72.6 mg/g). This was achieved by obtaining the biochar from mango peel, orange peel and corn husk by slow pyrolysis and modifying said biochar with MWNCTs by physisorption and ultrasonic cavitation. The purpose of this project consisted of the modification of biochar increases the capacity to adsorb CO_2 by at least 10%, which was corroborated by being subjected to a CO_2 chamber and verifying its adsorption with a CO_2 atmosphere meter. In conclusion, it can be mentioned that the adsorption capacity of corn husk biochar modified with multi-wall carbon nanotubes (BH-MWCNT's) increased by 123% for carbon dioxide.

Keywords: biochar; carbon nanotubes; CO_2 adsorption capacity; corn husk; pyrolysis.

Abbreviations

BC = Commercial biochar
BC-MWCNT's = Commercial biochar with MWCNT's
BH = Corn husk biochar
BH-MWCNT's = Biochar modified with multi-wall carbon nanotubes
BG = Biochar-graphene composites
BM = Mango peel biochar
BMNH = Complex mixed biochar
BN = Orange peel biochar
BN-MWCNT's = Orange peel biochar with MWCNT's
GHG = Greenhouse gas
PCMs = Phase-change materials

1. Introduction

The world is facing a major global environmental crisis. The increase in industrialization worldwide and the excessive use of non-renewable energy sources have resulted in a considerable emission of greenhouse gases. This uncontrolled emission has caused a rise in global temperature and therefore triggered a series of problems related to environmental degradation. From the pre-industrialization era, around the year 1850 until 2024, the global average concentration of carbon dioxide (CO_2) increased substantially from 285 to 424 ppm [1, 2]. Drafted to address the need for environmental change, the Paris Agreement establishes the requirement of a net-zero balance for greenhouse gas emissions by mid-century, to limit global warming to 1.5 °C [3, 4]. This situation involves reducing or removing CO_2 from the atmosphere by an additional 1100 million tons per year. To advance towards the goal of carbon neutrality and even achieve carbon negative, strategies and technologies are being developed (system maps, measurement techniques and light detection, among others) [5, 6]. Innovative materials such as MOFs, zeolites, cork, mycelium, green concrete, recycled polymers and biochar stand out for their adsorption and sustainability capabilities. We note that wood-derived materials continue being of an interest due to the possibilities to discover unusual properties [7].

MOFs (metal-organic framework structures) and zeolites, due to their high surface area and porosity, are extremely efficient in capturing CO_2, although their production is expensive and less sustainable. Cork, due to its natural porous structure, can passively adsorb gases or pollutants, while mycelium offers a lightweight and biodegradable alternative with adsorbent properties, ideal for specific applications. Green concrete and recycled polymers can be chemically modified to optimize gas capture, although their efficiency depends on the additives used. In comparison, biochar combines high porosity, adaptable chemical functionalization, and a carbon-negative production process, making it ecologically superior and economically viable [8]. In addition, unlike other materials, it can have multiple applications, from CO_2 capture [9, 10] to soil improvement, amplifying its positive impact on global sustainability.

Biochar, also known as black carbon, is a porous material that is formed from the thermal decomposition of biomass, such as crops, leaves, wood, bones, or manure, in the absence of oxygen [11, 12, 13]. This

pyrolysis process produces an organic solid material with carbon adsorption capacity, with temperatures typically not exceeding 700 °C [14]. The main components of biochar are carbon, hydrogen, oxygen, and nitrogen, with carbon accounting for more than 40% of the total. Unlike traditional coal (used as fuel), biochar is used for carbon storage and environmental applications. Biochar production involves three main stages. In the initial stage, the water is removed and the hydrocarbons are volatilized. In the intermediate stage, primary carbon is produced. In the final stage, the biochar slowly decomposes into solid waste with high fixed carbon content.

The carbon adsorption capacity of biochar and its mechanisms depends on activation, *i.e.*, on factors such as pyrolysis conditions (highlighting, temperature, heating rate and pressure) and activation methods without surface modification [15, 16, 17, 18, 19]. The main outstanding characteristics of biochar are as follows: 1) produced from waste, 2) can adsorb carbon on a large scale, 3) has a porous structure, a highly functionalized surface, 4) a supplier of nucleation sites, 5) compatible with polymers, 6) can hydrate cement, 7) has the ability to reduce noise by acoustic insulation, 8) can be a thermal insulator, act as immobilizers of pollutants, performing electromagnetic shielding, 9) has the ability to improve indoor air quality, self-healing capacity, among others. The nano form of biochar, referred to as *nanobiochar*, is a value-added product; it can absorb pollutants, microorganisms and nutrients better than biochar due to greater mobility in soils. There are various methodologies to modify the properties of biochar and nanobiochar, either chemically, physically, or biologically, by treating the feedstock or, more commonly, the biochar already produced [20, 21].

Biochar that exhibits a larger surface area and high porosity demonstrates considerable adsorption capacity [22, 23, 24, 25, 26]. The porous structure of biochar develops during pyrolysis, where the increase in dehydration leads to the formation of a porous surface. Biochar produced without an activation process will have a low surface area and lower porosity, so during the synthesis of biochar an activation process is involved to increase them. The activation process makes it possible to incorporate functional properties into biochar, intended for specific applications such as the adsorption of contaminants and the production of catalysts. The most common methods of altering the properties of biochar are physical activation and chemical activation. Physical activation focuses on the use of water vapor and gases (CO_2, N_2, NH_3 and O_2) at high temperatures. On the other hand, chemical activation encompasses acidic and alkaline modifications, as well as the addition of oxidation agents such as metal salts.

In additional to comprehensive review [27], several selected important studies on biochar and its composites are as follows. Thus, a metal-modified biochar as an economical and robust adsorbent for CO_2 capture was developed [28]. Using walnut shells, the authors synthesized the biochar by pyrolysis in a single step at different temperatures, followed by metal impregnation and heat treatment, making the magnesium-doped (Mg) biochar reaching the highest adsorption capacity, with 82.0 mg of CO_2 per gram. Comparatively, unmodified biochar showed an adsorption capacity of 72.6 mg/g, which demonstrates that the incorporation of Mg significantly improves its adsorbent properties, positioning walnut shell biochar as a promising and low-cost option for greenhouse gas mitigation.

Biochar derived from rice husks was studied as a smart material capable of loading nanonutrients and microorganisms [29]. To synthesize the biochar, authors employed a slow pyrolysis process in which they exposed the biomass to temperatures of 100, 200, 300, and 350°C for 24 hours, then added nanoparticles and microorganisms, and then characterized the material. The results showed that biochar acts as an efficient adsorbent and as a suitable carrier for microorganisms, showing great promise in applications within polymer technology. This study proposes a method for obtaining biochar from rice husks and presents its characterizations with a focus on polymeric applications. The production and characterization of biochar derived from coconut shell residues, varying the temperature in a range of 280-400 °C and the feeding of O_2 between 0-5% v/v during the pyrolysis reaction, was performed [30]. The study presents the experimental data obtained from each characterization, providing detailed information on the properties of biochar synthesized under different conditions. This work sets a benchmark for the synthesis of biochar from coconut shells, contributing to the development of materials derived from agricultural residues for environmental and adsorption applications.

Biochar and graphene (BG) composites were prepared using a one-step dip coating method and used them to remove phthalates from water [31]. According to the results, pyrolysis of the biochar-graphene compound at 600°C allows adsorption equilibrium to be reached within 48 hours. Adsorption kinetics revealed that the porous structure and surface properties of BG compounds regulate the adsorption rate of pollutant molecules, thus improving their performance. This method allowed the successful adhesion of graphene to the surface of the biochar, forming a composite material that effectively increases the specific surface area and porosity of the biochar, improving its adsorption capacity. Biochar derived from industrially derived oilseed kernel husk and its potential as a slow-release nitrogen-phosphate fertilizer and carbon sink was

prepared [32]. The authors carried out various characterizations of the biochar synthesized from this industrial biomass. The results showed that the carbon sequestration potential of palm kernel biochar, based on a 100-year period, is 0.398 t CO_2/t biomass. These finding positions biochar as a strategic product both for mitigating climate change and for the commercialization of carbon credits, highlighting its dual function as a fertilizer and contributor to carbon sequestration.

Hybrid biochar and carbon nanotube (CNT) composite materials for the encapsulation of phase-change materials (PCMs) and thermal energy storage were developed [33]. The biochar derived from bamboo was modified with CNT's using a hydrothermal method. The results showed that compounds with CNTs significantly improved latent heat storage capacity, reaching 152.3 J/g compared to 93.4 J/g for pure biochar. In addition, the composites demonstrated thermal stability and resistance to deformation, suggesting great potential for applications in low-temperature thermal energy storage. Applications of magnetic nanobiochar (MNBC) are known for use in environmental remediation and high-value applications [34]. Its synthesis begins with the transformation of biomass into biochar by slow pyrolysis, rapid pyrolysis, gasification, instant carbonization or torrefaction. The biochar is then converted into nanobiochar through ball milling, and finally transformed into MNBC by the magnetic precursor impregnation method. This work provides a variety of biochar synthesis definitions and techniques, contributing to knowledge about the manufacture of advanced materials for applications in the treatment of contaminants and other specialized uses. Finally, it was demonstrated that biochar production from waste could play a key role in the goal of reaching zero greenhouse gas (GHG) emissions in China by 2060 [35]. The authors examined the life cycle of GHG emissions under normal conditions and in three alternative scenarios, where burned crops were retained in the field, removed, or used to produce biochar. These results highlighted the capacity of biochar to act as a carbon sequestration material capable of reducing emissions from agricultural residues, thus contributing to the goal of carbon neutrality.

In this work, local-waste-derived biochar has been modified with multi-wall carbon nanotubes (MWNCT's) to develop a series of novel low-cost composites with a high carbon dioxide adsorption capacity. These composites are known to get important applications in various fields [36].

2. Experimental part

2.1. Materials and equipment

In the development of this project, the following high-purity reagents were used: multi-walled carbon nanotubes (MWCNT's; reactive grade, 98% purity, sizes 10-20 nm / 10-30 µm for both types; supplier *Nanostructured and Amorphous Materials, Inc.*), compressed nitrogen (N_2), reactive grade, 99% (*AOC Mexico*); isopropanol (C_3H_8O), reactive grade, 99% (*CTR Scientific*); sulfuric acid (H_2SO_4), reactive grade, 96.90% (*CTR Scientific*); sodium carbonate (Na_2CO_3), reactive grade, 99% (*Sigma-Aldrich*); and potassium bromide (KBr), reactive grade for FT-IR spectroscopy, ≥99% (*Sigma-Aldrich*). In addition, biomass samples (orange peel, mango peel, and corn husk), acquired at the *Operadora Merco, S.A.P.I. de C.V.* supermarket, located in Salinas Victoria (Mexico), and commercial biochar were used. Distilled water was also used for the different stages of the experimental process. Any organic matter with high carbon content can be used as biomass. To carry out this research, oranges, mangoes, and corn were purchased at the Merco commercial store, located in the municipality of Salinas Victoria, Nuevo León, Mexico, to use their peels as a source of biomass.

The obtained samples have been characterized by Fourier transform infrared spectroscopy (FTIR), model ThermoFisher Scientific NICOLET iS10, and by X-ray diffraction (XRD) in a Bruker D2 Phaser. Surface area measurements were carried out via nitrogen physisorption (BET) through a Micromeritics TriStar II Plus.

2.2. Husk extraction process

Initially, the orange, mango, and corn peels were washed to eliminate adhering residues, and cut into small pieces to facilitate drying. Each type of peel was processed separately: they were exposed to sunlight for 2 weeks and additionally placed in a drying oven at 100 °C for 3 h. The dried husks were then crushed in a rotational mill for 2 min and sifted to obtain a uniform particle size.

2.3. Pyrolysis process

10 grams of biomass were weighed and placed in an alumina crucible, which was introduced into the center of the tube furnace. To remove oxygen, the system was subjected to a nitrogen (N_2) atmosphere with a constant flow of 30 mL/min. The furnace was programmed for an initial temperature ramp to 100°C over a period of 10 min, with a residence time of 5 min, ensuring a nitrogen inert atmosphere. Subsequently, a second ramp was established: 45 min to 550°C, with a residence time of 2 h, allowing pyrolysis to be performed at a rate of 10°C/min. Finally, the oven was allowed to cool for 1.5 h. Once completed, the crucible was removed, and the sample was stored in a 16 mL vial. This procedure was carried out for biomass samples from mango peel, orange peel, corn husk, and a mixture of all three in equal

proportions.

2.4. Modification of waste-derived biochar with MWCNT's

A total of 0.5 g of synthesized biochar was weighed and transferred to a mortar. Then, 0.01 g of MWCNT's, equivalent to 2% of the biochar weight, was weighed, screened to the same particle size, and added to the mortar. We have chosen 2% MWCNT's loading (considered as low) in biochar due to 1) notably increased specific surface area at this concentration and good MWCNT's dispersion in the biochar matrix without MWCNT's agglomeration, caused by van der Waals forces, which could result blocade of pores and thus decrease adsorption performance, 2) enhanced mechanical stability and strength of the composite, 3) synergistic effects between adsorptive nanotube surfaces and functional groups of biochar (first of all, hydrophylic groups as –OH or –COOH), 4) high cost of MWCNT's obstaculizing their applications at higher scale (2% corresponds to optimal perfomance per unit cost).

Both components were ground together by mechanochemical grinding to facilitate their physisorption. The sample was stored in a 16 mL vial, to which 15 mL of isopropanol (C_3H_8O) was added. The vial was closed, labeled, secured with Parafilm paper, and then introduced into an ultrasound bath to enhance bonding between the biochar and the MWCNT's due to cavitation effects. We supposed that a synergic effect of the mechanochemical and ultrasonic treatments could result a better interaction of counterparts, giving priority to the second driving force for a better MWCNT dispersion. This process was carried out for 2 h, with pauses every 15 min to prevent water overheating. Finally, the isopropanol was evaporated by heating the vial in a 250 mL beaker filled with distilled water, on a heating plate at 150°C, within an extraction hood. The evaporation process lasted 1 h 15 min. The sample was then dried in an oven at 150°C for 3 h (Johnson et al., 2023).

Subsequently, the sample was uncovered, and the isopropanol was evaporated by heating in a water bath. This process consisted of placing the vial inside a 250 mL beaker with distilled water, which was placed on a heating plate at a temperature of 150°C, all inside an extraction hood. The evaporation process lasted approximately 1 h and 15 min. Finally, the sample was placed in the drying oven at 150°C for 3 h. This procedure was repeated for biochar derived from mango peel, orange peel, corn husk, and the mixed biochar. *Abbreviations*: BN (orange peel biochar), BN-MWCNT's (orange peel biochar with MWCNT's), BC-MWCNT's (commercial biochar with MWCNT's), BM (mango peel biochar), BH (corn husk biochar), BC (commercial biochar), BMNH (complex mixed biochar).

2.5. Modification of commercial biochar with MWCNT's

The commercial biochar was ground with a mortar, sifted, and subjected to the same pyrolysis and further conditions as the synthesized biochar to ensure uniform starting conditions.

2.6. Quantification of CO_2 adsorption capacity

The CO_2 adsorption capacity was analyzed for 10 samples: 4 of synthesized biochar modified with MWCNT's, 4 of synthesized biochar, 1 of commercial biochar modified with MWCNT's, and 1 of commercial biochar without treatment. CO_2 was synthesized from the reaction between 10% Na_2CO_3 aqueous solution and H_2SO_4. Prior to the adsorption experiment, the samples were degassed in an oven at 110°C for 4 hours. To quantify CO_2 adsorption, an air quality meter was used to measure the CO_2 concentration in parts per million (ppm). The meter and the closed sample vial were placed inside a large ziplock bag, which acted as a sealed chamber. To further minimize atmospheric gas interference, the bag was placed inside a Fisher Scientific Vadi-Vac pressure box, which generated a vacuum and reduced the amount of gas in the atmosphere. Once the box was opened, the ziplock bag was sealed promptly to prevent air entry.

Using a 10 mL syringe, 10 mL of CO_2 was extracted from a CO_2 bottle by inserting the needle through the balloon valve, taking advantage of its self-sealing properties. The CO_2 was injected into the bag, and an initial CO_2 concentration reading (in ppm) was recorded. With the bag sealed, the vial was then opened, allowing interaction between the CO_2 and the sample. After three minutes, a second CO_2 concentration reading was taken. Finally, the vial containing the sample was sealed and removed from the bag, and the sample was weighed three times on the analytical balance. The difference in mass before and after the adsorption process was used to determine the amount of CO_2 adsorbed by each sample. These repeated measurements ensured reliability and minimized random errors in the quantification process.

3. Results and discussion

3.1. FT-IR spectra

The comparison highlighted the structural and functional differences among the biochar types analyzed in Figure 1. The FTIR spectrum of mango peel biochar indicates a matrix rich in aromatic structures, with possible nitrile (C≡N) functional groups and some oxygenated residues like ethers and C-O groups. The pyrolysis of the biomass has converted much of the

cellulose and lignin into a carbonaceous material with stable aromatic rings, characteristic of biochar, imparting adsorption properties and chemical stability. The FTIR spectrum of orange peel biochar reveals structure rich in aromatic rings and oxygen and nitrogen residues, forming a stable carbonaceous material due to the thermal conversion of biomass during pyrolysis. This complex matrix provides potentially useful properties for adsorption and catalysis applications.

For corn husk biochar, the FTIR spectrum shows a significant proportion of aromatic rings and oxygenated groups such as esters and ethers. The presence of nitrile groups and conjugated bonds indicates that pyrolysis has generated a stable and resistant material. These characteristics suggest potential in adsorption and catalytic applications due to its chemical structure and functional group reactivity. Commercial biochar's FTIR spectrum shows structure rich in aromatic bonds and oxygenated compounds, with some nitrile and carbonyl group traces.

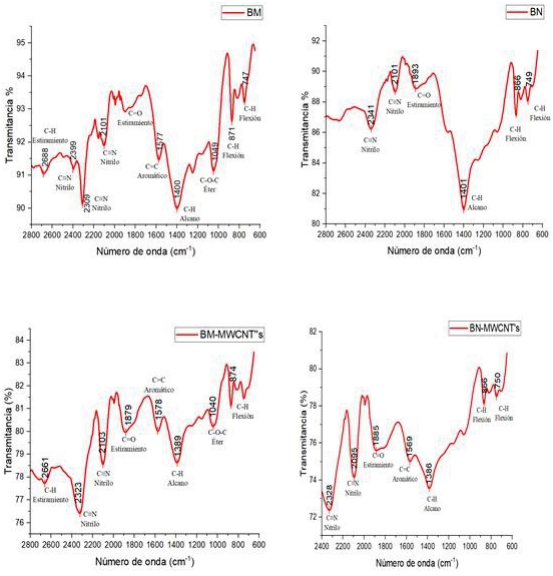

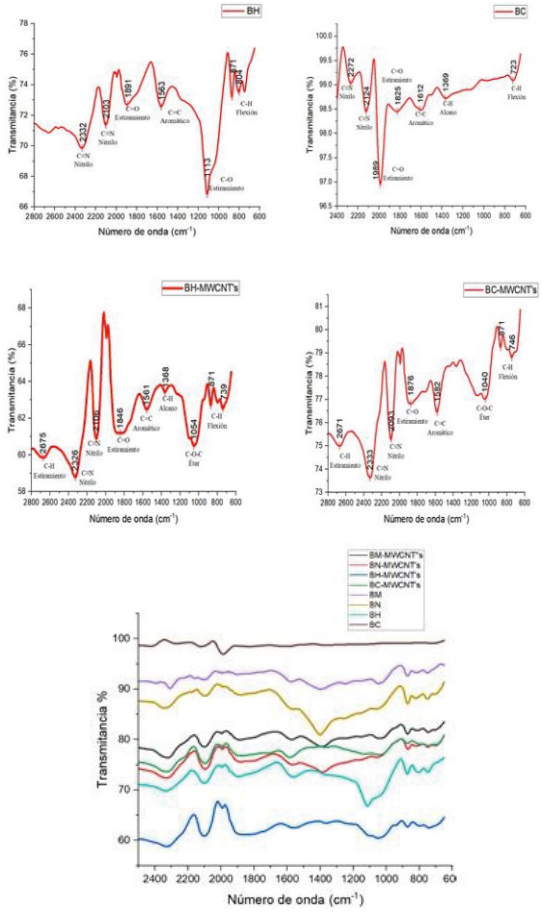

Fig. 1. FT-IR spectra of samples (x = wavelength cm^{-1}, y = transmittance, %).

The FTIR spectrum of MWCNT-modified mango peel biochar reveals carbonaceous structure rich in aromatic rings and oxygenated groups, with possible interactions between MWCNT's and biochar. The C≡N, C=C, and C-O bands suggest modification of biochar with carbon nanotubes improving its surface properties, potentially increasing adsorption capacity and reactivity; at the same time MWCNTs enable chemisorption (*e.g.*, π-π interactions). The FTIR spectrum of MWCNT-modified orange peel biochar displays structure rich in aromatic rings and oxygenated groups, indicating carbon nanotubes have influenced the carbonaceous network, enhancing its surface properties. Interactions between MWCNT's and biochar may improve adsorption capacity and reactivity, suitable for CO_2 capture, water treatment, or catalysis. The FTIR spectrum of MWCNT-modified corn husk biochar shows a structure composed of aromatic and oxygenated groups, suggesting carbon nanotubes have influenced the carbon lattice. The modifications could improve adsorption properties and surface reactivity, making it suitable for CO_2 capture, water treatment, or catalysis. For MWCNT-modified commercial biochar, the FTIR spectrum shows the

introduction of oxygenated functional groups like carbonyls, esters, and ethers, enhancing adsorption and surface reactivity properties. The aromatic structure of the original biochar is largely maintained, making this modified material suitable for CO_2 capture, water treatment, or catalysis.

3.2. CO_2 adsorption

To conduct the experiment, ten samples of approximately 0.35 grams each one were prepared and heated in an oven at 110°C for four hours. These samples were then exposed to a CO_2 atmosphere and analyzed using two methods: gravimetry, employing an analytical balance to determine the adsorption capacity in mg of CO_2 per gram of biochar (mg CO_2/g biochar), and by changes in CO_2 concentration within a closed atmosphere using an air quality meter to assess the amount of CO_2 adsorbed in parts per million (ppm CO_2). These results are shown in Figure 2, Table 1 and 2.

Table 1. Adsorption capacity of biochar in mg CO_2/g biochar.

Sample	$\bar{x}$ Initial	$\bar{x}$ Final	mg CO_2 / g biochar
BC	0.3510	0.3528	5.2237
BM	0.3501	0.3538	10.5684
BN	0.3498	0.3523	6.9557
BH	0.3498	0.3587	25.6361
BMNH	0.3590	0.3608	5.2001
BC-MWCNT's	0.3582	0.3624	11.7253
BM-MWCNT's	0.3515	0.3594	22.4751
BN-MWCNT's	0.3481	0.3530	14.0751
BH-MWCNT's	0.3471	0.3669	57.2416
BMNH-MWCNT's	0.3504	0.3544	11.4144

($\bar{x}$ is an average value from several parallel experiments)

Table 2. CO_2 adsorption capacity (ppm) by biochar.

Sample	CO_2 *initial* (*ppm*)	CO_2 *final* (*ppm*)	CO_2 adsorbed (*ppm*)
BC	1220	1171	49
BM	978	935	43
BN	2075	2045	30
BH	1407	1372	51
BMNH	980	949	31
BC-MWCNT's	1055	888	167
BM-MWCNT's	2051	1317	734
BN-MWCNT's	1245	1114	131
BH-MWCNT's	1037	732	305
BMNH-MWCNT's	1572	1482	90

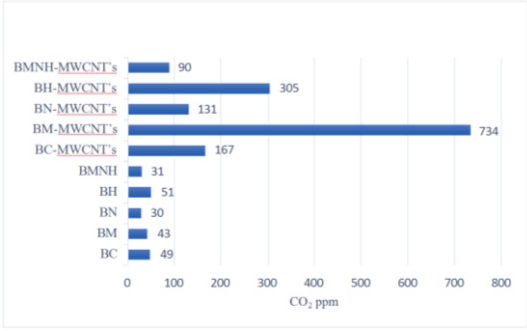

Fig. 2. CO_2 adsorption results.

3.3. XRD results

Figure 3 below presents the results obtained from the X-ray diffraction (XRD) analysis performed on the synthesized and modified biochar samples. This analysis allows us to identify the crystalline phases present and evaluate the crystallinity of the samples. The diffraction patterns obtained were compared with standard databases to determine the mineralogical composition and structural characteristics.

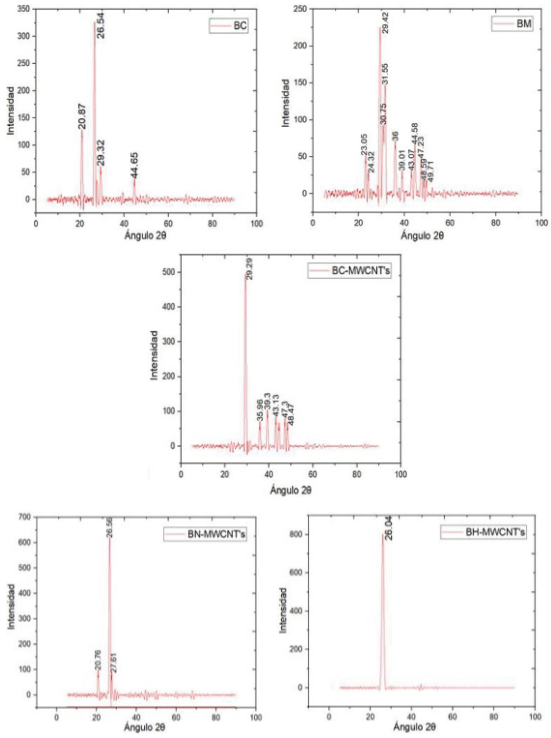

Fig. 3. XRD diffractograms (x = 2θ angle, y = Intensity).

The most significant peaks and their correlation with the corresponding crystal phases can provide a detailed overview of the structure of biochar. Figure 4 presents a comparison of the diffractogram peaks of each sample analyzed.

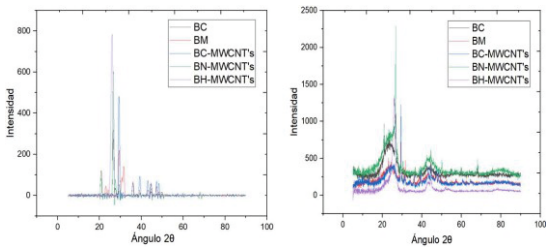

Fig. 4. XRD comparative diffractograms (x = 2θ angle, y = Intensity).

To analyze the peaks obtained in the diffractogram, it is essential to compare them with a crystallographic database. Table 3 presents some references related to the crystalline phases commonly found in biochar.

Table 3. XRD crystallographic references [30].

Angle 2θ	Crystallographic form
Wide peak at ~24(002)	Graphite-like structure (turbostatic carbon, amorphous)
Wide beak at ~42 (100)	Graphite-like structure (turbostatic carbon, amorphous)
Sharp and intense peaks at ~26, ~44 and ~55 (101) and less acute peak at ~60	Graphite (crystal)

In MWCNT-modified biochar samples (BC-MWCNT's, BN-MWCNT's and BH-MWCNT's), an increase in peak intensity to 26° is observed compared to unmodified biochar. This suggests that the incorporation of MWCNT's has contributed to an increase in the overall crystallinity of the material. In addition, the peak located at 44° is characteristic of crystalline graphite, specifically of the plane (100). Its presence in the synthesized biochar reinforces the idea that the material contains crystalline components, suggesting that the crystallinity of the biochar could have been increased due to the incorporation of MWCNT's. To corroborate the data obtained from the X-ray diffractogram, the percentage of crystallinity was calculated using the ratio between the area under the peaks corresponding to the crystalline regions and the total area of the diffractogram, multiplied by 100. The results obtained are presented in Table 4 and show notable differences between the analyzed samples.

Table 4. Crystallinity of samples.

Sample	Crystallinity
BC	28.75%
BM	22.95%
BC-MWCNT's	30.81%
BN-MWCNT's	35.84%
BH-MWCNT's	47.14%

3.4. BET results

This section presents the results obtained from the analyses carried out on the different types of biochar: BN (orange peel biochar), BN-MWCNT's (orange peel biochar with MWCNT's) and BC-MWCNT's (commercial biochar with MWCNT's). These were characterized by using the BET nitrogen adsorption technique to determine their surface and structural properties, such as surface area, pore volume and pore size distribution. In addition, the BJH, DFT and NLDFT models were used to obtain a detailed evaluation of porosity in different size and volume ranges. The BET results obtained for each property are presented in Table 5.

Table 5. BET results.

Property	BN	BC-MWCNT's	BN-MWCNT's
Surface Area (BET)	148.71 m^2/g	192.80 m^2/g	204.17 m^2/g
Total Pore Volume (Adsorption)	0.1116 cm^3/g	0.1359 cm^3/g	0.1222 cm^3/g
Total Pore Volume (Desorption)	0.1116 cm^3/g	0.1359 cm^3/g	0.1222 cm^3/g
Average Pore Diameter (BET)	3.0017 nm	2.8185 nm	2.3946 nm
Average Pore Diameter (BJH)	5.3655 nm	5.2148 nm	3.8827 nm
Volume (DFT, ≤10.935 nm)	0.10030 cm^3/g	0.12518 cm^3/g	0.12019 cm^3/g
Area (DFT, ≥9,445 nm)	5.929 m^2/g	5.987 m^2/g	2.994 m^2/g
Volume (NLDFT,	0.10516 cm^3/g	0.12814 cm^3/g	0.11377 cm^3/g

≤99.993 nm)			
Area (NLDFT, ≥2,399 nm)	12.682 m^2/g	13.801 m^2/g	11.007 m^2/g

The adsorption-desorption isotherm is presented in Figure 5, which shows the results obtained during the BET analysis.

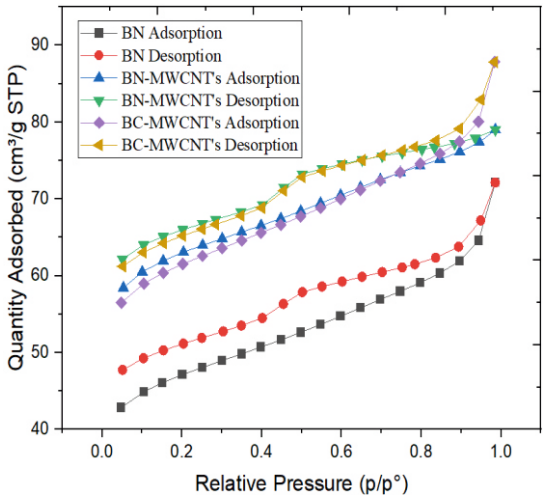

Fig. 5. Adsorption-desorption isotherms.

The adsorption-desorption isotherm of orange peel (BN) biochar shows a remarkable adsorption capacity, with an adsorbed amount that increases as the relative pressure (P/P_0) increases, reaching a value close to 75 cm^3/g STP, which indicates that BN has an effective porous structure to capture gases on its surface. However, the desorption curve reaches higher values than the adsorption curve at similar relative pressures, suggesting hysteresis behavior. This phenomenon is characteristic of mesoporous materials, due to capillary condensation in the pores. The hysteresis loop confirms that the material has a complex porous structure, suitable for high-adsorption applications such as gas capture or contaminant removal.

Adsorption-desorption isotherm for orange peel biochar with multi-wall carbon nanotubes (BN-MWCNT's) shows that, as the relative pressure increases, the amount of gas adsorbed also increases, evidencing that BN-MWCNT's has a good ability to adsorb gas in its porous structure. The desorption curve, although it follows a similar pattern to the adsorption curve, presents slightly higher values at the same relative pressures, which generates a hysteresis loop. This behavior is indicative of the presence of mesopores, where the gas condenses and does not completely desorb when the pressure decreases, which is due to capillary forces in the pores. The maximum adsorption capacity, which reaches around 80 cm^3/g STP, highlights the material's efficiency in gas adsorption.

The adsorption-desorption isotherm of commercial biochar with multiwall carbon nanotubes (BC-MWCNT's) shows a characteristic behavior of mesoporous materials, evidenced by the hysteresis loop present between the adsorption and desorption curves. As the relative pressure (P/P_0) increases, the amount of gas adsorbed increases consistently, reaching a maximum of 90 cm^3/g STP, demonstrating excellent adsorption capacity. The observed hysteresis suggests the existence of mesopores where capillary condensation occurs, a common phenomenon in materials with heterogeneous porous structures. The shape of the isotherm confirms that BC-MWCNT's has a well-developed pore network with varied sizes, optimizing its capacity to retain gases. BN-MWCNT's and BC-MWCNT's stand out for their more pronounced hysteresis bonds compared to BN, indicating a greater number of mesopores and a more developed porous structure. This behavior is attributed to the integration of multi-walled carbon nanotubes (MWCNT's), which increase the specific surface area and provide additional active sites for CO_2 adsorption. Its tubular structure and high surface-to-volume ratio optimize both diffusion and the capture of molecules, favoring more efficient adsorption. In addition, the physical and chemical interactions of MWCNT's, such as van der Waals forces, significantly strengthen biochar's ability to capture gases, highlighting its potential in adsorption applications.

4. Conclusions and further outlook

Based on the results obtained, it is concluded that biochar demonstrates excellent adsorption properties due to its textural characteristics, and structural modifications can significantly enhance its performance. Among the synthesized biochars, the adsorption capacity followed the order BH > BM > BC > BN, with the modified samples exhibiting similar trends. Notably, BH-MWCNT's achieved a CO_2 adsorption capacity of 57.24 mg CO_2/g biochar, a 123% increase compared to BH's 25.64 mg CO_2/g biochar. Furthermore, the BH-MWCNT samples showed a measurable adsorption capacity of 305 ppm CO_2, a 498% improvement over BH's 51 ppm CO_2. XRD characterization revealed an increase in crystallinity due to modifications, with a 47.14% enhancement in the intensity of (100) and (101) planes in BH-MWCNT. BET analysis confirmed that BC-MWCNT outperformed BN-MWCNT in nitrogen adsorption capacity (90 cm^3/g STP *vs*. 80 cm^3/g STP) and demonstrated higher pore volume in smaller ranges. However, the adsorption efficiency of BC-MWCNT and BN-MWCNT was comparable to BN, indicating limitations in the MWCNT modification process. The

modification of biochar with MWCNT's derived from natural products increased CO_2 adsorption by more than 10%, validating the project hypothesis.

BH-MWCNT (containing cellulose in BH as main component, hemicellulose, and lignin) is shown to outperform other feedstocks (fruit peel-derived biochar containing more acidic functional groups) in the CO_2 adsorption due to the following characteristics (Liu et al, 2024): 1) more basic surface groups (C=O, COO^-, -OH, among others) (Janu et al, 2021) which react with CO_2 having an acidic nature, 2) the presence of basic-nature silica and ash in BH and Na^+/K^+ content in fruit peels decreasing porosity under pyrolysis, 3) higher stability of corn husk and much lower stability of fruit peels allowing varying pyrolysis conditions in a broader range in the first case, 4) large surface area and well-developed pore structure of BH-derived biochar. At the same time, macropores, micropores, and mesopores in the fruit peels-derived biochar provide certain contribution to their adsorption capacity [37]. In whole, CO_2 adsorption capacity of biochar depends on presence of heteroatoms and basic functional groups, micropore volume and area, surface area, among other factors.

To optimize future work, it is recommended to increase the biochar and solvent volumes to enhance MWCNT integration and the cavitation effect during ultrasonication. The quantity of MWCNT's used for modification should also be carefully considered, and triplicate measurements should be performed to confirm CO_2 adsorption capacities.

5. Acknowledgments

The authors are grateful to the Universidad Autónoma de Nuevo León for the help providing access to necessary equipment.

6. References

[1]. Cheng, H. Future Earth and Sustainable Developments. *The Innovation*. 2020, *1*(3), 100055.

[2]. Klaaßen, L.; Stoll, C. Harmonizing corporate carbon footprints. *Nat. Commun*. **2021**, *12*(1), 1-13.

[3]. Haszeldine, R.; Flude, S.; Scott, V. Negative emissions technologies and carbon capture and storage to achieve the Paris Agreement commitments. *Phil. Trans. R. Soc. A*. **2018**, *376*(2119), 20160447. https://doi.org/10.1098/rsta.2016.0447.

[4]. Yang, W.; Min, Z.; Yang, M.; Yan, J. Exploration of the Implementation of Carbon Neutralization in the Field of Natural Resources under the Background of Sustainable Development—An Overview. *Int. J. Environ. Res*. **2022**, *19*(21), 1-28.

[5]. Kharissova, A.B.; Kharissova, O.V.; Kharisov, B.I.; Peña Méndez, Y. Carbon negative footprint materials: A review. *Nano-Struct. Nano-Objects*. **2024**, *37*, 101100. doi: 10.1016/j.nanoso.2024.101100.

[6]. Chen, L.; Msigwa, G.; Yang, M. Strategies to achieve a carbon neutral society: a review. *Environ. Chem. Lett*. **2022**, *20*, 2277-2310.

[7]. Gao, H.; Li, Y.; Xie, Y.; Liang, D.; Li, J.; Wang, Y.; Xiao, Z.; Wang, H.; Gan, W.; Pattelli, L.; Xu, H. Optical wood with switchable solar transmittance for all-round thermal management. *Composites Part B: Engineering*. **2024**, *275*, 111287.

[8]. Rajendran, A.; Sakthivel, A.; Dong, Z.; Li, W. What makes biochar an interesting CO_2 adsorbent? *Frontiers of Chemical Science and Engineering*, **2024**, *19*, article number 12.

[9]. Zhang, C.; Ji, Y.; Li, C.; Zhang, Y.; Hu, Y.; Jiang, L.; Wu, C. The Application of Biochar for CO_2 Capture: Influence of Biochar Preparation and CO_2 Capture Reactor. *Ind. Eng. Chem. Res*. **2023**, *62*(42), 17168–17181.

[10]. Zhang, Y.; He, M.; Wang, L.; Yan, J.; Ma, B.; Zhu, X. et al. Biochar as construction materials for achieving carbon neutrality. *Biochar*. **2022**, *4*, 59.

[11]. Ghazali, M.S.M.; Zaini, M.S.M.; Arshad, M.; Syed-Hassan, S.S.A. Co-production of biochar and carbon nanotube from sewage sludge in a two-stage process coupling pyrolysis and catalytic chemical vapor deposition. *Waste Disposal & Sustainable Energy*, **2024**, *6*, 323–334.

[12]. Xue, Q; Xie, S; Zhang, T. Biochar production and modification for environmental improvement. In: *Biochar in Agriculture: Achieving Sustainable Development Goals*. **2022**, 181-191. doi: 10.1016/B978-0-323-85343-9.00025-2.

[13]. Yaashikaa, R.; Senthil Kumar, P.; Varjani, S.; Saravanan, A. A critical review on the biochar production techniques, characterization, stability and applications for circular bioeconomy. *Biotechnol Rep (Amst)*. **2020**, *28*, 1-15.

[14]. Jagnade, P.; Panwar, N.L. Experimental investigation on the performance of activated bamboo biochar for CO_2 and PM2.5 adsorption. *Emergent Mater*. **2024**, *7*, 1227–1238. doi: 10.1007/s42247-024-00624-1.

[15]. Cao, D.; Niu, R.; Mo, G.; Deng, H.; Liu, R.; Fan, J. Adsorption properties and competitive adsorption mechanism exhibited by carbon-nanotube-modified biochar for removal of crude oil and Ni(II) pollutants from water. *Ecotoxicology and Environmental Safety*, **2025**, *290*, 117557.

[16]. Kwon, C.W.; Tae, S.; Mandal, S. Comparative Analysis of CO_2 Adsorption Performance of Bamboo and Orange Peel Biochars. *Molecules* **2025**, *30*(7), 1607.

[17]. Hassan, R.; Baghban, A. Predicting CO_2 adsorption in KOH-activated biochar using advanced machine learning techniques. *Scientific Reports*, **2025**, *15*, Article number: 24410.

[18]. Janu, R.; Mrlik, V.; Ribitsch, D.; Hofman, J; Sedláček, P.; Bielská, L.; Soja, G. Biochar surface functional groups as affected by biomass feedstock, biochar composition and

pyrolysis temperature. *Carbon Resources Conversion*, **2021**, *4*, 36-46.

19]. Li, Y.; Yu, H.; Liu, L.; Yu, H. Application of co-pyrolysis biochar for the adsorption and immobilization of heavy metals in contaminated environmental substrates. *J. Hazard. Mater*. **2021**, *420*, 126655.

[20]. Yan, J.; Zhang, M.; Chen, X.; Chen, C.; Xu, X.; Jiang, S. Multi-walled carbon nanotubes modified corn straw biochar as high-performance anode in microbial fuel cells. *J. Environ. Chem. Eng*. **2024**, *12*(5), 113316. doi: 10.1016/j.jece.2024.113316.

- [21]. Zhang, X.; Xu, H.; Xiang, W.; You, X.; Dai, H.; Gao, B. Lignin-impregnated biochar assisted with microwave irradiation for CO_2 capture: adsorption performance and mechanism. *Biochar*, **2024**, *6*, article number 22.
- [22]. Lodhi, N.; Chadar, S.N.; Thakur, D.S.; Raikwar, A. A Comprehensive Study on Biochar-Based Nanocomposites in Removal of Organic Pollutants from Wastewater. J. Water Environ. *Nanotechnol*. **2024**, *9*(3), 302-317.
- [23]. Alfei, S.; Zuccari, G. Carbon-Nanotube-Based Nanocomposites in Environmental Remediation: An Overview of Typologies and Applications and an Analysis of Their Paradoxical Double-Sided Effects. *J. Xenobiot*. **2025**, *15*(3), 76.
- [24]. Fan, Y.; Su, J.; Xu, L.; Liu, S.; Hou, C.; Liu, Y.; Cao, S. Removal of oxytetracycline from wastewater by biochar modified with biosynthesized iron oxide nanoparticles and carbon nanotubes: Modification performance and adsorption mechanism. *Environmental Research*, **2023**, *231*(3), 116307.
- [25]. Guo, S.; Li, Y.; Wang, Y.; Wang, L.; Sun, Y.; Liu, L. Recent advances in biochar-based adsorbents for CO_2 capture. *Carbon Capture Science & Technology*. **2022**, *4*, 100059. doi:10.1016/j.ccst.2022.100059. Available from: https://www.sciencedirect.com/science/article/pii/S2772656822000306.
- [26]. Liu, T.; Fan, X.; Wu, K.; Tao, C.; Bai, X.; Sun, X. Structural characteristics of biochars made from different parts of corn straw and their adsorption performances for methylene blue. *Journal of Water Process Engineering*, **2024**, *68*, 106562.
- [27]. Dissanayake, P.D.; You, S.; Deshani Igalavithana, A.; Xia, Y.; Bhatnagar, A.; Gupta, S.; Wei Kua, H.; Kim, S.; Kwon, J.H.; Tsang, D.C.W.; Ok, Y.S. Biochar-based adsorbents for carbon dioxide capture: A critical review. *Renewable and Sustainable Energy Reviews*, **2020**, *119*, 109582.
- [28]. Lahijani, P.; Mohammadi, M.; Mohamed, A.R. Metal incorporated biochar as a potential adsorbent for high capacity CO_2 capture at ambient condition. *J. CO_2 Util*. **2018**, *26*, 281-293.
- [29]. Hassan, A.; Mahmoud, W.; Turky, G.; Safwat, G. Rice husk derived biochar as smart material loading nano nutrients and microorganisms. *Bulg. J. Agric. Sci*. **2020**, *26*(2), 309-322.
- [30]. Castilla-Caballero, D.; Barraza-Burgos, J.; Gunasekaran, S.; Roa-Espinosa, A.; Colina-Márquez, J.; Machuca-Martínez, F.; et al. Experimental data on the production and characterization of biochars derived from coconut-shell wastes obtained from the Colombian Pacific Coast at low temperature pyrolysis. *Data Br*. **2020**, *28*, 104855.
- [31]. Yu, Z.; Wang, W.; Gao, H.; Liang, D. Properties Analysis and Preparation of Biochar–Graphene Composites Under a One-Step Dip Coating Method in Water Treatment. *Appl. Sci*. **2020**, *10*(11), 3689.
- [32]. Domínguez, E.; Uttran, A.; Loh, S.; Manero, M.; Upperton, R.; Tanimu, M.; et al. Characterisation of industrially produced oil palm kernel shell biochar and its potential as slow release nitrogen-phosphate fertilizer and carbon sink. *Mater. Today Proc.* **2020**, *31*(1), 221-227.
- [33]. Atinafu, D.G.; Wi, S.; Yun, B.Y.; Kim, S. Engineering biochar with multiwalled carbon nanotube for efficient phase change material encapsulation and thermal energy storage. *Energy*. **2021**, *216*, 119294. doi:10.1016/j.energy.2020.119294.
- [34]. Sonowal, S.; Koch, N.; Sarma, H.; Prasad, K.; Prasad, R. A Review on Magnetic Nanobiochar with Their Use in Environmental Remediation and High-Value Applications. *J. Nanomater*. **2023**, *2023*, 4881952.
- [35]. Xia, L.; Cao, L.; Yang, Y.; et al. Integrated biochar solutions can achieve carbon-neutral staple crop production. *Nat. Food*. **2023**, *4*, 236–246. Available from: https://doi.org/10.1038/s43016-023-00694-0.
- [36]. Kumar, R. Carbon Nanotube Coated Biochar-Based Composites and Their Applications. In: Bhawani, S.A.; Jawaid, M.; Alotaibi, K.M. (eds), *Biochar-based Composites. Composites Science and Technology*. Springer, Singapore. **2025**, 131–148.
- [37]. Hussin, F.; Kheireddine Aroua, M.; Szlachta, M. Biochar derived from fruit by-products using pyrolysis process for the elimination of Pb(II) ion: An updated review. *Chemosphere*, **2022**, *287*(3), 132250.